

FLUID BED DRYING AS UPGRADING TECHNOLOGY FOR FEASIBLE TREATMENT OF KOLUBARA LIGNITE

by

Milić D. ERIĆ^a, Milan B. STAKIĆ^{a*}, and Miloš J. BANJAC^b

^a Laboratory for Thermal Engineering and Energy, Vinca Institute of Nuclear Sciences,
University of Belgrade, Belgrade, Serbia

^b Faculty of Mechanical Engineering, University of Belgrade, Belgrade, Serbia

Original scientific paper
DOI: 10.2298/TSCI150725172E

An overview of the current status of low-rank coal upgrading technologies is presented in the paper, particularly with respect to drying and dewatering procedures. In order to calculate the significant parameters of the moisture removal process, a model of convective coal drying in a fluid bed, based on the two-phase (bubbling) fluidization model proposed by Kunii and Levenspiel, is developed and presented. Product-specific data (intraparticle mass transfer, gas-solid moisture equilibrium) related to the particular coal variety addressed here (Kolubara lignite) are obtained through preliminary investigations. Effective thermal conductivity of the packed bed as defined by Zehner/Bauer/Schlunder is used to define heat transfer mechanisms occurring in the suspension phase of the fluid bed. A completely new set of experimental data obtained has been successfully used to validate the model additionally.

Key words: *low-rank coal, moisture removal, drying coefficient, fluid bed*

Introduction

Based on energy strategy it is expected that lignite (low-rank coal) will continue to be the main energy source used in Serbian power plants, mainly due to the fact that it is the most abundant and cheapest fossil fuel available. Lignite in particular, with its deposits found and extensively exploited in Serbia (as well as in many other European countries) is characterized by relatively low sulfur content, with moisture content of 25-70% and low energy output. The presence of moisture in coal reduces coal friability, negatively affecting the quality of grinding, as well as pneumatic transport of pulverized coal. Reduced moisture level in coal results in increased power plant efficiency, reduced ash disposal requirements and reduced pollutant emissions. On the other hand, upgrading processes used to reduce the moisture content in coal cause an increase in combustion temperatures, due to the higher calorific value achieved at the expense of reduced moisture. There are several options to reduce moisture content of low-rank coals. The methods used may be divided into two main groups: conventional evaporative drying (direct or indirect dryers, packed or fluid bed dryers, rotary kiln, etc.) and non-evaporative dewatering processes (mechanical thermal expression, hydro-thermal dewatering, etc.).

The main objective of the work presented in this paper is to provide a brief overview of the current status of low-rank coal upgrading technologies, particularly addressing utiliza-

* Corresponding author; e-mail: mstakic@vinca.rs

tion of drying technologies, as well as to propose appropriate calculation method for evaluating parameters of the coal pre-drying process. The packed bed drying model was developed in the past and validated for biological materials [1-4], but also successfully used to depict drying of Kolubara lignite [5]. The paper reflects on possible upgrades of this model so as to be suitable for simulation of the fluid bed drying process. Product-specific kinetic data *drying coefficient* and equilibrium data (moisture isotherms) of the solids (lignite) are derived from a very small-scale experiments [6], while heat and mass transfer coefficients, indicative for heat and mass transfer phenomena between a solids surface and surrounding gas in a packed bed (*e. g.* in the solids-gas suspension of the fluid bed), $\alpha_{s,G}$ and $\beta_{s,G}$, being dependent on internal structure of the dried solids, are expressed in general terms, using non-dimensional correlations and applying the Zehner, Bauer and Schlunder model [7].

Removal of moisture from low-rank coal

The most commonly used procedures for reduction of moisture content in low-rank coals may be classified into two categories, according to the basic principle of moisture removal [8, 9]:

(1) Drying procedures:

- Flue gas mills: (a) Drying with hot flue gases, (b) Drying with cold flue gases.
- Fluid bed dryers: (a) heated air (moderately – up to 80 °C) [10, 11], (b) inert gases (nitrogen, *etc.*) dryers, (c) superheated steam (SHS) dryers:
 - DWT (Dampf Wirbelschicht Trocknung), steam fluid bed drying,
 - WTA (Wirbelschicht Trocknung mit interner Abwärmennutzung), fluid bed drying with internal heat recovery, performed at atmospheric pressure,
 - DDWT (Druckaufgeladene Dampf-Wirbelschicht-Trocknung), steam fluid bed drying with internal heat recovery, performed under high pressure (up to 6 bar).
- Other dryers: (a) high pressure pneumatic dryers, (b) steam heated rotary tube dryers, (c) Fleissner drying procedure (combined SHS and air treatment),

(2) Dewatering procedures:

Mechanical dewatering – centrifugal dehydration, mechanical thermal expression (MTE) process [12-16], hydro-thermal dewatering process [17-20].

Energy consumption related to mentioned procedures is presented in tab. 1 and fig. 1.

It is noticeable that dewatering procedures usually require less energy than conventional drying procedures. Still, the SHS drying processes (Fleissner, WTA) are also characterized by lower energy consumption compared to other drying procedures, while the fluid bed SHS drying with heat recovery, *i. e.* WTA drying, developed by RWE Power AG, certainly has the lowest energy consumption of all coal drying technologies. Use of SHS for coal drying has a number of advantages, including: (1) improved safety through reduced risk of explosion or fire (non-oxygen gas), (2) significant reduction in dust emission, (3) increased drying rates and thermal efficiency, and (4) improved coal grinding ability.

Consequently, particular attention is paid to fluid bed dryers, which are enabling intensive contact between fluidization gas (hot air, flue gases or steam) and solids (material being dried). Gas flow-rate has to be such sufficient that pressure-drop, needed to achieve the required state of fluidization (to overcome particle weight and bring the particles in the state of levitation), is reached. Fluidization gas also acts as a drying agent (supplies energy required for drying and removes evaporated moisture). In case that steam (water vapor) is used as fluidization gas, flow-rate of the gas stream leaving the fluid bed needs to be higher so as to compensate for evaporated water. It is possible to make additional use of this steam (after

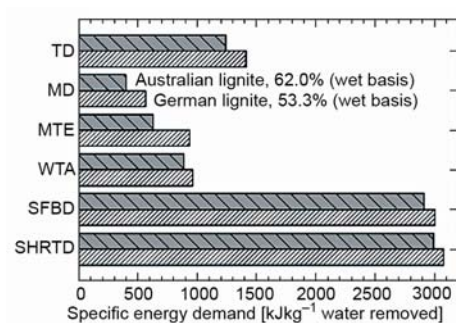


Figure 1. Specific energy demand for water removal using different drying technologies [9]; TD – thermal dewatering, MD – mechanical dewatering, MTE – mechanical thermal expression, WTA – steam fluid bed dryer with internal heat recovery, SFBD – steam fluid bed dryer, SHRTD – steam heated rotary tube dryer

Table 1. Comparison of energy consumption for various coal dryers [21]

Dryer type	Energy consumption [kJkg ⁻¹ water removed]
Rotary dryer	3700
Rotary tube dryer	2950-3100
Chamber dryer	3150
Pneumatic dryer	3100
Fluid bed dryer	3100-4000
Fleissner process SHS	1300-1750
Fluid bed dryer SHS with heat recovery (WTA)	450

being appropriately treated in order to remove impurities) by means of: (1) recirculation – back into the fluid bed, (2) condensation – in a heat exchanger (where steam would give up its latent heat during condensation), or (3) recompression – utilization as overheated steam. Energy can be supplied into the fluid bed by means of the heaters (tubes with hot gas or steam flowing inside) immersed in the bed.

Modeling of convective drying

It is well known that conventional evaporative convective drying involves complex transport phenomena mixed up in three consecutive processes. The first one is moisture (liquid) movement in solids, occurring from the wet interior towards the gas-solid interface (internal pore, particle surface, *etc.*). This process is slower in larger solids and/or materials with low moisture content. The second one is evaporation facilitated by heat (energy) supplied either externally or taken from the solids and used to transform liquid into vapor. The last one is vapor movement to the surrounding gas by diffusion and convection. The slowest of the processes will determine the drying rate. Prediction of falling-rate drying kinetics by theory alone is very difficult and accurate small-scale experiments are required instead. It is possible to estimate drying rates under different conditions by applying concepts such as the *characteristic drying curve*, [22, 23], *etc.*, or the *drying coefficient*, [24, 25], *etc.*

Much work has been done to model and analyze both continuous and batch fluid bed dryers [26-36]. Each of the models developed has its own specificity, but with a common feature of utilizing the fluidized state specific heat and mass transport coefficients. This paper, however, presents an exclusive mathematical model developed to describe heat and mass transfer between solid, gas, and bubble phases, based on the two-phase (bubbling) fluidization model proposed by Kunii and Levenspiel [37]. The model rests on the basic idea that heat and mass transfer between gas and particles (*i. e.* the drying process) in suspension phase, as in the case of packed bed of particles, may be calculated using the *drying coefficient* approach, carrying out calculations for the elementary layers (volumes) and using the general expressions for the entire bed. The influence of particle mixing, taking place in mobile beds (fluid bed, vibrated fluid bed, rotary bed, *etc.*), induced by bubble flow in the fluid bed, is related to the dif-

fusion term in respective differential equations and is taken into account through reported particle diffusion coefficients [37].

General equation

Differential equations describing conservation of general dependent variable, Φ , in case of an unsteady problem, can be expressed in the general form, as proposed by Patankar [38]:

$$\frac{\partial}{\partial \tau} (\rho \Phi) + \text{div} (\bar{u} \rho \Phi) = \text{div} (\Gamma_{\Phi} \text{grad} \Phi) + S_{\Phi} \quad (1)$$

The terms seen in eq. (1) are denoted as the *unsteady term*, the *convection term*, the *diffusion term*, and the *source term*, respectively. Expressions for general diffusion coefficient, Γ_{Φ} , and the source term, S_{Φ} , depend on the physical meaning of the variable Φ . In convective drying, moisture content, X , and enthalpy (*i. e.* temperature, T_S) of the material being dried, as well as humidity, Y , and enthalpy (*i. e.* temperature, T_G) of the used drying agent, represent particular cases of the general dependent variable to be determined.

Packed bed model

With the intention to analyze convective drying in a packed bed, an unsteady-state 1-D mathematical model, already validated for different biological materials (corn grains, soybean, potato cubes, poppy seeds, *etc.*, see [1-4]), was developed in the past. This model, describing simultaneous heat and mass transfer between the gas phase and the dried product during convective drying in a packed bed, rests upon the following assumptions:

- drying parameters vary in 1-D only, namely in a direction of gas flow (usually vertical), and only changes of the parameters in this direction are addressed and discussed,
- all solids are of the same size, shape, and density at one moment in time,
- the gas-solid interface is at thermodynamic equilibrium,
- the product drying rate is calculated by applying the *drying coefficient* principle, and
- dispersion of mass or heat in the considered gas flow direction is neglected.

In order to define heat and mass balances the system of partial differential equations can be written applying the eq. (1) and implementing the assumptions mentioned [5, 39].

Fluid bed model

Fluid bed model describes principally the heat and mass transfer phenomena taking place between solid, gas, and bubble phases. It is based herein on the two-phase (bubbling) fluidization model developed by Kunii and Levenspiel [37]. In accordance with this model, initial mass flow-rate of the gas phase is divided into a portion flowing through the suspension phase, assuming that suspension phase is at the state of minimum fluidization, and another portion (excess gas) flowing through the bubble phase. The basic approach in this work is to calculate heat and mass transfer rates between gas and solid particles (*i. e.* the drying process) in the suspension phase, such as in the case of packed bed of particles, making it possible to upgrade the packed bed model into the fluid bed model.

Besides the assumptions made for the packed bed model, fluid bed model rests upon the following additional assumptions:

- the suspension phase is in the state of minimum fluidization (considered as a packed bed),
- the excess gas is flowing through the bubble phase (particle-free gas),
- bubbles are of the same size and uniformly distributed across the one cross-section,

- every uprising bubble drags the solids in its wake, causing the dragged solid particles to sink back through the suspension phase, in that manner causing mixing of the solids, and
- gas generated by moisture evaporation from the particle surface is distributed through the bubble phase, causing different size of bubbles to form in the uprising cross-sections of the bed.

Consequently, a system of partial different equations derived based on eq. (1) and adjusted to the case of convective drying in a fluid bed can be written:

Conservation of moisture in bubble phase (particle-free gas)

$$\frac{\partial}{\partial \tau} (M_{G,B,d} Y_B) + \frac{\partial}{\partial z} (u_{G,B} M_{G,B,d} Y_B) = M_{G,B,d} (K_{BE})_B (Y_E - Y_B) \quad (2)$$

Conservation of moisture in suspension phase

gas:
$$\frac{\partial}{\partial \tau} (M_{G,E,d} Y_E) + \frac{\partial}{\partial z} (u_{G,E} M_{G,E,d} Y_E) = M_{G,B,d} (K_{BE})_B (Y_B - Y_E) + \dot{M}_m \quad (3)$$

solids:
$$\frac{\partial}{\partial \tau} (M_{S,d} X) + \frac{\partial}{\partial z} (u_S M_{S,d} X) = \frac{\partial}{\partial z} \left(M_{S,d} D_{\text{eff}} \frac{\partial u_S}{\partial z} \right) - \dot{M}_m \quad (4)$$

Conservation of enthalpy, bubble phase

$$\frac{\partial}{\partial \tau} (M_{G,B,d} c_B T_B) + \frac{\partial}{\partial z} (u_{G,B} M_{G,B,d} c_B T_B) = V_B (H_{BE})_B (T_E - T_B) \quad (5)$$

Conservation of enthalpy, suspension phase

gas:
$$\frac{\partial}{\partial \tau} (M_{G,E,d} c_E T_E) + \frac{\partial}{\partial z} (u_{G,E} M_{G,E,d} c_E T_E) =$$

$$= V_B (H_{BE})_B (T_B - T_E) + \alpha_{S,G} a_b V (T_S - T_E) + c_v (T_E - T_S) \dot{M}_m \quad (6)$$

solids:
$$\frac{\partial}{\partial \tau} (M_{S,d} c_S T_S) + \frac{\partial}{\partial z} (u_S M_{S,d} c_S T_S) = \frac{\partial}{\partial z} \left(V_S \lambda_{\text{eff}} \frac{\partial T_S}{\partial z} \right) +$$

$$+ \alpha_{S,G} a_b V (T_E - T_S) - r \dot{M}_m \quad (7)$$

Equation of continuity for gas phase

$$\frac{\partial}{\partial \tau} M_G + \frac{\partial}{\partial z} (u_G M_G) = \dot{M}_m \quad (8)$$

Initial gas phase mass flow-rate, $\dot{M}_{G,\text{in}}$, can be divided, according to the two-phase (bubbling) fluidization model, into a portion flowing through the bubble phase, \dot{M}_B , and a portion flowing through the suspension phase, \dot{M}_E :

$$\dot{M}_{G,\text{in}} = A \rho_G u_{G,\text{in}} = \dot{M}_B + \dot{M}_E = A f_B \rho_G u_{G,B} + A (1 - f_B) \rho_G u_{G,E} \quad (9)$$

where $u_{G,\text{in}}$ is the superficial velocity *i. e.* the gas velocity in a free cross-section of the bed and A and f_B are bubble phase volume fraction. Then, gas velocity through the suspension phase, $u_{G,E}$, and through the bubble phase, $u_{G,B}$, can be obtained from: $u_{G,E} = u_{G,\text{mf}}/\psi_{\text{mf}}$, and $u_{G,B} = u_{G,\text{in}}/f_B - u_{G,E}(1 - f_B)/f_B$.

The suspension phase is in the state of minimum fluidization and can be approximated by a packed bed having the bed void fraction [37]:

$$\psi_{mf} = 0.586\phi_s^{-0.72} \left[\frac{\eta_G^2}{\rho_G(\rho_s - \rho_G)g d_s^3} \right]^{0.029} \left(\frac{\rho_G}{\rho_s} \right)^{0.021} \quad (10)$$

As in the case of fluid bed (as well as the packed bed), there is no directed movement of the solids, meaning that the solids velocity is set to $u_s = 0$.

Dispersion coefficient of the solids can be calculated [37]:

$$D_{eff} = \frac{k^2 \psi_{mf}}{3f_B u_{G,mf}} d_B (u_{G,in} - u_{G,mf})^2 \quad (11)$$

where d_B is the bubble diameter defined [40]:

$$d_B = 0.54(u_{G,in} - u_{G,mf})^{0.4} (h + 4\sqrt{A_0})^{0.8} g^{-0.2} \quad (12)$$

where h is the height of the bubble (*i. e.* cross-section of the bed) above the fluid bed inlet zone, and A_0 is the cross-section of the opening, which represents a characteristic of flow distributor.

It is important to note that a system of partial differential equations for the case of convective drying in a packed bed can be easily obtained from already presented eqs. (2)-(8) by means of:

- (1) removal of eq. (2) and (5) – being related to the bubble phase,
- (2) simplification of eq. (3) and (6) by deleting the *source terms* related to the bubble phase, having $(K_{BE})_B$, *i. e.* $(H_{BE})_B$,
- (3) simplification of eq. (4) and (7), by deleting the *diffusion terms* (having D_{eff} , *i. e.* λ_{eff}) – absence of solids dispersion in a packed bed.

Source terms

Moisture transport from the interior to the surface of the solids is a more complex phenomena due to variety of involved mechanisms (capillarity, diffusion, thermal diffusion, bulk and molecular flow, surface diffusion) that depend on the structure of the product involved.

The moisture flow-rate from the interior to the surface of the solids is expressed empirically:

$$\dot{M}_m = M_{S,d} k_i (X_{sf,eq} - X) \quad (13)$$

where k_i is the internal moisture transport coefficient (the already mentioned *drying coefficient*).

Moisture transported from the interior to the surface of the solids has to be subsequently transferred to the surrounding gas. It is assumed that the solid surface and the gas in its immediate vicinity are in the state of hygroscopic equilibrium. Therefore, the flow-rate of evaporated moisture can also be expressed:

$$\dot{M}_m = M_{G,d} \beta_{S,G} a_b (Y - Y_{eq}) \quad (14)$$

Since eq. (13) and (14) are coupled by the state of equilibrium, they have to be solved simultaneously. The unknown variables Y_{eq} and $X_{sf,eq}$ (equilibrium gas solids and moisture content at the solid surface, respectively) must meet the hygroscopic equilibrium requirement for specific moisture level on the surface of a specific product. The empirical drying coefficient, k_i , must also be specified for the particular product considered. On the other hand, the gas-side mass transfer coefficient, $\beta_{S,G}$, may be obtained from general, non-product-specific equations.

Parameter estimation

Due to the complex water-solid bonding mechanisms, the equilibrium between a certain material and air at a given temperature (sorption isotherm) can only be determined experimentally, and is usually correlated empirically. For this purpose, the empirical relationship proposed by Stefanović *et al.* [6]:

$$1 - \varphi_{eq} = e^B \quad (15)$$

where

$$\varphi_{eq} = \frac{P_{at}}{P_{sat}} \frac{Y_{eq}}{Y_{eq} + (1 - Y_{eq}) \frac{\tilde{M}_V}{\tilde{M}_G}}$$

and

$$B = -B_0 T_S^a X_{eq}^b \quad (16)$$

with T_S expressed in K is used.

The same authors [6] have proposed an expression for the internal moisture transport coefficient (drying coefficient) k_i from eq. (13) that accounts for the overall resistance to moisture transport in the material, namely:

$$k_i = A_K d_S^{n_D} \frac{X}{X_0} T_S^{n_T} \quad (17)$$

with T_S in °C and d_S in m.

All parameters in eq. (16) (B_0 , a , b) were determined during preliminary investigations [6], for the same type of Kolubara coal using a well-known static equilibration method applied for the small specimen of salt solutions oversaturated with air. The parameters obtained were later used in measurement of sorption isotherms that were then correlated based on eq. (15) and shown in fig. 2. Drying kinetics experiments, carried out by the same authors, were performed in very thin beds (only one or two particle layers) comprised of 5.1 mm and 20 mm diameter coal pieces with moisture content of 0.02 kg/kg and 0.04 kg/kg, using air at temperatures between 60 °C and 200 °C and with flow velocities of 1 m/s and 2 m/s. Air parameters can be assumed to remain approximately constant during its flow through thin layers described, thereby enabling the parameters

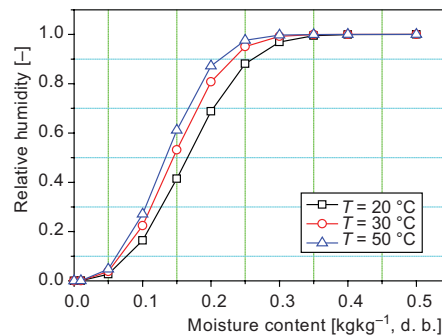


Figure 2. Moisture isotherms for Kolubara lignite

in eq. (17) (A_K, n_D, n_T) to be derived directly, compared with [41]. All product-specific parameters of hygroscopicity and coal particle-side drying kinetics are summarized in tab. 2.

Table 2. Parameters of sorption equilibria, eq. (16), and drying kinetics, eq. (17), for lignite [6]

Kinetics			Equilibria		
A_K , after eq. (14)	n_D , [-]	n_T , [-]	B_0 , after eq. (12)	a , [-]	b , [-]
0.0005	-1.2	3.3	-14.027	0.62	2.7

Opposite to the previously discussed coefficients, the heat and mass transfer coefficients describing phenomena occurring between particle surface and gas in a packed bed (suspension phase of fluid bed as well), $\alpha_{S,G}$ and $\beta_{S,G}$, do not depend on the internal structure of the product. As reported in the literature, they have been investigated extensively and are generally expressed in terms of suitable non-dimensional correlations, which can be defined on the basis of transport characteristics discussed later on.

Transport characteristics

Thermal conductivity of the packed bed

Effective thermal conductivity of the packed bed (λ_b), can be consistently defined from the model after Zehner, Bauer and Schlunder [7]:

$$k_b = \frac{\lambda_b}{\lambda_F} \quad (18)$$

$$k_b = 1 - \sqrt{1 - \psi} + \sqrt{1 - \psi} k_c \quad (19)$$

with

$$k_c = \frac{2}{N} \left(\frac{B}{N^2} \frac{k_S - 1}{k_S} \ln \frac{k_S}{B} - \frac{B + 1}{2} - \frac{B - 1}{N} \right), \quad B = 1.25 \left(\frac{1 - \psi}{\psi} \right)^{10/9},$$

$$N = 1 - \frac{B}{k_S}, \quad k_S = \frac{\lambda_S}{\lambda_F}$$

Prevailing heat transfer mechanism

Transient thermal breakthrough in porous media (*i. e.* packed bed) is generally influenced by the additive mechanisms [42].

(1) Axial heat transfer (A_1)

$$A_1 = \frac{(1 + K^*)^2}{\text{Pe}_S} \frac{\lambda_{ax}}{\lambda_F}, \quad (20)$$

with: $\lambda_{ax}/\lambda_F = \lambda_b/\lambda_F + \text{Pe}_S/2$, $K^* = (1 - \psi)/\psi \cdot (\rho c)_S/(\rho c)_F$, $\text{Pe}_S = u_{G,in}(\rho c)_F \cdot d_S/\lambda_F$, where λ_{ax} denotes thermal conductivity in axial (fluid flow) direction, ρ and c in $(\rho c)_F$ and $(\rho c)_S$ represent density and specific heat capacity of the fluid and the solids, respectively, d_S is equivalent diameter of the solids, and Pe_S is Peclet criterion.

(2) Fluid-to-solids heat transfer (A_2)

$$A_2 = \frac{K^{*2} Pe_S}{Nu_S a_b d_S} \quad (21)$$

where a_b is bed specific surface area, and Nusselt criterion can be obtained from Gnielinski [43]:

$$Nu_S = 2 + \sqrt{Nu_{lam}^2 + Nu_{turb}^2} \quad (22)$$

with

$$Nu_{lam} = 0.664 \sqrt[3]{Pr} \sqrt{Re_S}, \quad Nu_{turb} = \frac{0.037 Re_S^{0.8} Pr}{1 + 2.443 Re_S^{-0.1} (\sqrt[3]{Pr^2} - 1)}$$

(3) Heat transfer inside the solids (A_3):

$$A_3 = \frac{K^{*2} Pe_S}{60(1 - \psi) \frac{\lambda_S}{\lambda_F}} \quad (23)$$

It is convenient to jointly address previously described heat transfer effects, by defining the equivalent Nusselt criterion:

$$Nu_S^* = \frac{K^{*2} Pe_S}{(A_1 + A_2 + A_3) a_b d_S} \quad (24)$$

The gas-side heat transfer coefficient, $\alpha_{S,G}$, is calculated then from the expression:

$$\alpha_{S,G} = \frac{Nu_S^* \lambda_G}{d_S} \quad (25)$$

Definitions of mass transfer mechanisms are similar to those describing the heat transfer mechanisms, but characterized by corresponding effective diffusion coefficient, δ_{eff} , and *molecular* Peclet criterion $Pe_S^D = u_{G,in} d_S / \delta_{eff}$. For example, axial mass dispersion, D_{ax} , is obtained from the expression:

$$\frac{D_{ax}}{\delta} = \frac{\delta_{eff}}{\delta} + \frac{Pe_S^D}{2} \quad (26)$$

Minimum fluidization velocity

Minimum fluidization velocity, $u_{G,mf}$, can be calculated from:

$$u_{mf} = Re_{S,mf} \frac{\eta_G}{\rho_G d_S} \quad (27)$$

where $Re_{S,mf} = (\kappa_1^2 + \kappa_2 Ar_S)^{0.5}$, with [44] $\kappa_1 = 24$, $\kappa_2 = 0.049$.

Numerical procedure

A numerical procedure based on a method developed by Patankar [38] has been used to solve the partial differential equations. Equations (2)-(8) are discretized using the control-volume method, *i. e.* the packed bed, while the fluid bed is divided into a finite number of control volumes by utilizing a vertical grid. The iterative line-by-line method is used to solve

the linearized algebraic equations, with recurrence formula applied to calculate the variable corresponding to every line. The same procedure was then implemented for all the lines in one direction. This method, called the Thomas algorithm or the tri-diagonal-matrix algorithm, is described in detail by Patankar [38].

Calculation procedure starts with the first control volume and is continued for the adjoining control volume, when looking in the gas flow direction (axial direction of the bed), but only after the balance preconditions, specified by eqs. (2)-(8), are met. The fact that there is no directed movement of the solids inside the packed and/or the fluid bed ($u_s = 0$), *i. e.*, the absence of *convection terms* in eqs. (4) and (7), does not affect calculation of the height-dependent variation of solid moisture content and enthalpy, but creates some numerical, stability-related problems. In spite of this, convergent solutions could always be obtained through appropriate selection of under-relaxation factors [38].

Validation of packed bed model

The packed bed model was validated in the past by measuring equilibria and single-particle – or equivalent (thin layer) – drying kinetics, fitting the product-dependent model parameters, simulating the deep-bed drying of the material considered and comparing the calculated results with respective experimental data for the case of different biomaterials, including corn grains, corn on the corn-cob, wheat grains, poppy seeds, potato cubes, *etc.* [2-4]. The same type of validation has been carried out for coal. The product-dependent parameters have been taken from [6], as presented in tab. 2.

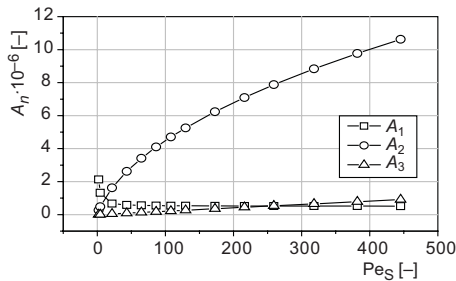


Figure 3. Influence of axial heat transfer (A_1), heat transfer between solid and gas phase (A_2), and intra-solids heat transfer (A_3) for the packed bed of coal particles, calculated on the basis of the properties of lignite particles given in tab. 3

gas) prevails for common values of Peclet criterion related parameter ($u_{G,in} > 1.0$ m/s). The particular transfer mechanisms are jointly addressed through the equivalent Nusselt criterion specified in the eq. (24) and utilized in the model.

Table 3. Properties of lignite particles

$d_{S,d}$, [mm]	$\rho_{S,d}$, [kgm ⁻³]	ρ_b , [kgm ⁻³]	$c_{S,d}$, [kJkg ⁻¹ K ⁻¹]	λ_s , [Wm ⁻¹ K ⁻¹]	ψ , [-]	\square_s , [-]	u_{mf} , [ms ⁻¹]
1.5, 2.57	1250	600.0	1.55	0.058	0.52	0.7	0.7, 1.1

The respective data have been systematically compared with results obtained using the model developed in the course of the work presented herein. Example of data comparison is published in [5, 39].

Validation of fluid bed model

A completely new set of experimental data was obtained using Sherwood fluid bed dryer apparatus. Mentioned apparatus was upgraded with parallel measurement equipment in

order to check additionally data obtained from original apparatus. The Kolubara coal (lignite) samples having granulation from 1.5 mm to 4 mm and initial moisture content about 1.0 were dried applying hot air with inlet temperatures from 60-20 °C and inlet velocities from 0.6 m/s to 3.1 m/s. Comparison of simulation and experimental data for the case of fluid bed coal drying (obtained results for only two types of coal particles, with properties given in tab. 3) is presented in figs. 4 and 5.

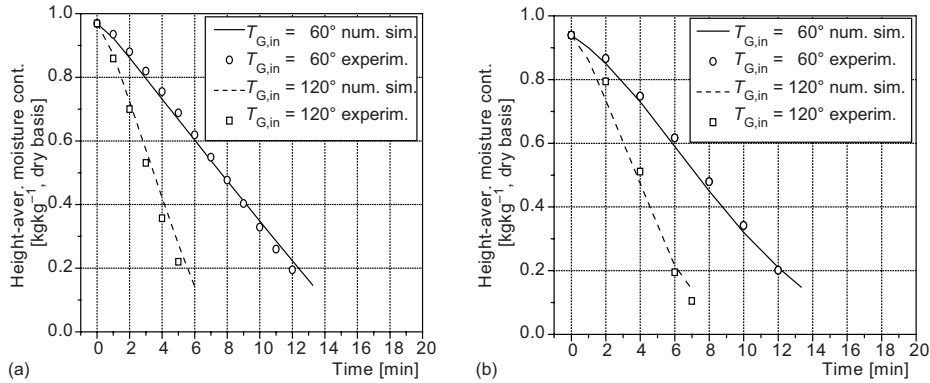


Figure 4. Simulated and experimentally determined lignite drying kinetics in a fluid bed; $Y_{in} = 0.008$, $u_{G,in} = 1.9$ m/s, $M_{S,0} = 0.21$ kg; (a) $d_{S,d} = 1.5$ mm, $X_0 = 0.969$, (b) $d_{S,d} = 2.57$ mm, $X_0 = 0.939$

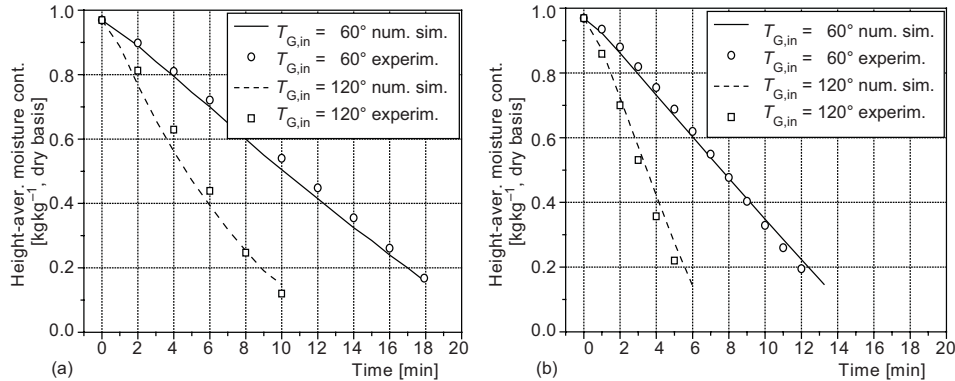


Figure 5. Simulated and experimentally determined lignite drying kinetics in a fluid bed; $Y_{in} = 0.008$, $d_{S,d} = 1.5$ mm, $X_0 = 0.969$, $M_{S,0} = 0.21$ kg; (a) $u_{G,in} = 1.2$ m/s, (b) $u_{G,in} = 1.9$ m/s

Effect of particle size and air inlet temperature

It is obvious that the drying should be faster for the case of smaller coal pieces, because of smaller intraparticle resistance, eq. (13), and because of the superior specific surface area causing a more intensive moisture transport from the material surface to the surrounding air, eq. (14), but it was not perceptibly pronounced for low granulation used in the recent experiments (fig 4). The key explanation should be the observed additional grinding of coal particles during experiment. On the other hand, drying is faster in the case of higher air temperature due to superior difference between the partial pressure of water vapour (air humidity) at the material surface and the partial pressure of water vapour in the surrounding air (air humidity), eqs. (14)-(17).

In both cases, calculations/experiments were carried out down to the predetermined final moisture content of approx. 0.2. Certainly, the coal could be dried to the final moisture content lower than this value, down to a limiting final value set by the equilibrium moisture content, which is dependent on the parameters of the air contacting the material. Prolonged coal drying in order to reach the equilibrium moisture content, from the point of view of the economics of the entire process, including subsequent combustion, makes not much sense. In addition, coal leaving the drier continues to dry, and is going to lose additional few percent of its moisture content.

Effect of air flow-rate

In fig. 5 the changes of coal moisture content (height-averaged) with time, obtained by experiment and simulation, are shown for the case of a coal diameter (1.5 mm) and for two extreme inlet air temperatures (60 °C and 120 °C) for two given air velocities (1.2 m/s and 1.9 m/s). On the basis of the experiments and numerical calculations, it can be concluded that the lower air flow-rate, *i. e.* inlet air velocity, will induce longer drying time. It is obvious that the drying should be faster for the case of higher air velocities, because of the higher gas-side heat transfer coefficient, $\alpha_{S,G}$, eq. (25), as long as there is a sufficient moisture content at the solids surface.

Conclusions

- An overview of the current status of low-rank coal upgrading technologies, particularly with respect to exploitation of drying procedure is presented. Typical methods used nowadays to reduce moisture content of coal are concisely described. Comparison of energy consumption in case of different coal dryers, as well as some aspects of the SHS drying process, with particular consideration of low-rank coal drying specifics, is given.
- A mathematical model originally developed for packed bed drying of biomaterials is briefly explained. With respect to the results presented in this paper it should be pointed out that the model was originally developed for conventional convective drying, where wet cold materials are dried by the means of preheated air, but it was also successfully used for a somewhat non-typical convective coal drying process applied after a high-pressure steam drying treatment, where already heated material is dried and cooled using ambient air [5].
- A fluid bed drying model and respective numerical procedure are described in detail. The model is developed in order to explore the influence of drying agent (hot air, SHS, *etc.*) parameters (temperature, humidity, flow-rate) and material-related parameters (particle size) on the coal drying process, as well as to test drying process efficiency. The properties of lignite particles used both in experiments and simulation are defined (tab. 3). Necessary parameters associated with single-particle drying kinetics and sorption equilibria of the considered coal variety (lignite – tab. 2) were verified and used in calculations performed. A comparison of simulated and experimentally determined height-averaged lignite drying kinetics in a fluid bed is given and discussed.

The future work will be focused at the investigation (experimental and numerical) of new possibilities of reduction of energy consumption, similar to, for example, the new self-heat recuperation technology proposed by Aziz *et al.* [45].

Acknowledgment

The authors would like to acknowledge the Ministry of Education, Science and Technological Development of the Republic of Serbia for its input (Research projects TR33050 and III42010) along the course of preparing this publication.

Nomenclature

A	– cross-section of the bed, [m ²]
a, b	– exponents of eq. (16)
A_1	– axial heat transfer as defined by eq. (20)
A_2	– fluid-to-solids heat transfer as defined by eq. (21)
A_3	– heat transfer inside the solids as defined by eq. (23)
a_b	– bed specific surface area, [m ² m ⁻³]
A_K	– coefficient with dimensions as defined by eq. (17)
B_0	– coefficient with dimensions as defined by eq. (16)
c	– specific heat capacity, [Jkg ⁻¹ K ⁻¹]
d	– diameter, [m]
D	– dispersion coefficient of solids, [m ² s ⁻¹]
f	– volume fraction
g	– acceleration of gravity (=9.81 ms ⁻²)
h	– bed height, [m]
$(H_{BE})_B$	– overall volumetric heat transfer coefficient between bubble and suspension based on volume of bubbles [Wm ⁻³ K ⁻¹] [37]
k	– diffusion coefficient (= 0.15)
k_b	– relative thermal conductivity defined by eq. (18)
k_i	– internal mass drying coefficient, [s ⁻¹]
$(K_{BE})_B$	– overall coefficient of gas interchange between bubble and suspension based on volume of bubbles [s ⁻¹] [37]
M	– mass, [kg]
\dot{M}	– mass flow-rate, [kgs ⁻¹]
\bar{M}	– molecular mass, [kgkmol ⁻¹]
n_D, n_T	– exponents in eq. (17)
p	– pressure, [Pa]
r	– heat of evaporation, [Jkg ⁻¹]
S_ϕ	– general source term as defined by eq. (1)
T	– temperature, [°C, K]
u	– velocity, [ms ⁻¹]
\bar{u}	– velocity vector
V	– volume, [m ³]
X	– material moisture content (dry basis), [-]
Y	– gas moisture content (dry basis), [-]
z	– axial co-ordinate, [m]

Greek symbols

α	– heat transfer coefficient, [Wm ⁻² K ⁻¹]
β	– mass transfer coefficient, [ms ⁻¹]
Γ_ϕ	– general diffusion coefficient as defined by eq. (1)
δ	– diffusion coefficient, [m ² s ⁻¹]
η	– dynamic viscosity, [Pa·s]
λ	– thermal conductivity [Wm ⁻¹ K ⁻¹]
ρ	– density, [kgm ⁻³]
ϕ	– relative air humidity, [-]
ϕ	– sphericity of particulate solids, [-]
Φ	– general dependent variable, [-]
ψ	– bed void fraction, [-]
τ	– time, [s]

Dimensionless criteria

Ar_S	– Archimedes criterion, $d_S^3 \rho_S (\rho_S - \rho_G) g / \eta_G^2$, [-]
Nu_S	– Nusselt criterion, $\alpha_{S,G} d_S / \lambda_G$, [-]
Pe_S	– Peclet criterion, $[= u_{G,in} (\rho c)_F d_S / \lambda_F]$
Pr	– Prandtl criterion, $c_G \eta_G / \lambda_G$, [-]
Re_S	– Reynolds criterion, $d_S u_G \rho_G / \eta_G$, [-]

Subscripts

at	– atmosphere
ax	– axial
b	– bed
B	– bubble, bubble phase
d	– dry
E	– suspension phase
eff	– effective
eq	– equilibrium
F	– fluid
G	– gas
i	– internal
in	– inlet
L	– liquid
lam	– laminar
m	– moisture
mf	– minimum fluidization
S	– solids
sat	– saturated
sf	– surface
turb	– turbulent
V	– vapor
0	– initial, superficial

References

- [1] Stakić, M., Stefanović, M., Numerical Simulation of Corn Drying in Fixed Bed, *Agricultural Engineering, 1* (1995), 1-2, pp. 17-25
- [2] Stakić, M., Numerical Simulation of Real Materials Convective Drying in Fixed Bed, *Thermal Science, 1* (1997), 2, pp. 59-70
- [3] Stakić, M., Numerical Study on Hygroscopic Capillary-Porous Material Drying in a Packed Bed, *Thermal Science, 4* (2000), 1, pp. 25-41

- [4] Stakić, M., Tsotsas, E., Model-Based Analysis of Convective Grain Drying Process, *Drying Technology*, 23 (2005), 9-11, pp. 1895-1908
- [5] Stakić, M., Tsotsas, E., Modeling and Numerical Analysis of an Atypical Convective Coal Drying Process, *Drying Technology*, 22 (2004), 10, pp. 2351-1373
- [6] Stefanović, M., et al., Investigation of Convective Drying of the Kolubara Lignite and its Quality (in Serbian), *Proceedings*, Coal Usage in Thermal-Energetic Symposium, Belgrade, 1983
- [7] Tsotsas, E., *VDI-Warm-Atlas* (in German), 9th ed., Section Dee 9, Springer, Berlin, 2002
- [8] Karakas, E., et al., Computer Simulation Studies for the Integration of an External Dryer into a Greek Lignite-Fired Power Plant, *Fuel*, 81 (2002), 5, pp. 583-593
- [9] Jumah, R. Y., et al., *Control of Industrial Dryers. Handbook of Industrial Drying* (Ed. A. S. Mujumdar), 2nd ed., Marcel Dekker, New York, USA, 1995
- [10] Sarunac, N., et al., One Year of Operating Experience with a Prototype Fluidized Bed Coal Dryer at Coal Creek Generating Station, *Proceedings*, 3rd International Conference on Clean Coal Technologies for Our Future, Cagliari, Italy, 2007
- [11] Hyun-Seok, K., et al., Fluidized Bed Drying of Loy Yang Brown Coal with Variation of Temperature, Relative Humidity, Fluidization Velocity and Formulation of its Drying Rate, *Fuel*, 105 (2013), Mar., pp. 415-424
- [12] Bergins, C., Science and Technology of the Mechanical/Thermal Dewatering, Habilitation, University Dortmund, Dortmund, Germany, 2005
- [13] Bergins, C., Kinetics and Mechanism During Mechanical Thermal Dewatering of Lignite, *Fuel*, 82 (2003), 4, pp. 355-364
- [14] Bergins, C., Mechanical/Thermal Dewatering of Lignite. Part 2: A Rheological Model for Consolidation and Creep Process, *Fuel*, 83 (2004), 3, pp. 267-276
- [15] Hulston, J., et al., Physico-Chemical Properties of Loy Yang Lignite Dewatered by Mechanical Thermal Expression, *Fuel*, 84 (2005), 14-15, pp. 1940-1948
- [16] Bergins, C., et al., Mechanical/Thermal Dewatering of Lignite. Part 3: Physical Properties and Pore Structure of MTE Product Coals, *Fuel*, 86 (2007), 1-2, pp. 3-16
- [17] Allardice, D. J., et al., The Characterisation of Different Forms of Water in Low Rank Coals and Some Hydrothermally Dried Products, *Fuel*, 82 (2003), 6, pp. 661-667
- [18] Favas, G., Jackson, W. R., Hydrothermal Dewatering of Lower Rank Coals, 1. Effects of Process Conditions on the Properties of Dried Product, *Fuel*, 82 (2003), 1, pp. 53-57
- [19] Favas, G., Jackson, W. R., Hydrothermal Dewatering of Lower Rank Coals, 2. Effects of Coal Characteristics for a Range of Australian and International Coals, *Fuel*, 82 (2003), 1, pp. 59-69
- [20] Favas, G., et al., Hydrothermal Dewatering of Lower Rank Coals, 3. High Concentration Slurries from Hydrothermally Treated Lower Rank Coals, *Fuel*, 82 (2003), 1, pp. 71-79
- [21] Karthikeyan, M., et al., Low-Rank Coal Drying Technologies – Current Status and New Developments, *Drying Technology*, 27 (2009), 3, pp. 403-415
- [22] Meel, D. A. van., Adiabatic Convection Batch Drying with Recirculation of Air, *Chemical Engineering Science*, 9 (1959), 1, pp. 36-44
- [23] Tsotsas, E., Measurement And Modeling Of Intraparticle Drying Kinetics: A Review, *Proceedings*, 8th International Drying Symposium (IDS '92), Montreal, Canada, 1992, pp. 17-41
- [24] Luikov, A. V., *Drying Theory* (in Russian), 1st ed., Energiya, Moscow, 1968
- [25] Milojević, D. Ž., Stefanović, M., Convective Drying of Thin and Deep Beds of Grain, *Chemical Engineering Communication*, 13 (1982), 4-6, pp. 261-269
- [26] Palancz, B., A Mathematical Model for Continuous Fluidized Bed Drying, *Chemical Engineering Science*, 38 (1983), 7, pp. 1045-1059
- [27] Lai, F. S., et al., Modelling and Simulation of a Continuous Fluidized-Bed Dryer, *Chemical Engineering Science*, 41 (1986), 9, pp. 2419-2430
- [28] Li, M., Duncan, S., Dynamical Model Analysis of Batch Fluidized Bed Dryers, *Particle & Particle Systems Characterization*, 25 (2008), 4, pp. 328-344
- [29] Wang, H. G., et al., Modelling of Batch Fluidized Bed Drying of Pharmaceutical Granules, *Chemical Eng. Science*, 62 (2007), 5, pp. 1524-1535
- [30] Wang, H. G., et al., Investigation of Batch Fluidized Bed Drying by Mathematical Modelling, CFD Simulation and ECT Measurement, *AIChE Journal*, 54 (2007), 2, pp. 427-444
- [31] Groenewold, H., Tsotsas, E., A New Model for Fluid Bed Drying, *Drying Technology*, 15 (1997), 6-8, pp. 1687-1698

- [32] Temple, S. J. van Boxtel, A. J. B., Modelling of Fluidized-Bed Drying of Black Tea, *Journal of Agricultural Engineering Research*, 74 (1999), 2, pp. 203-212
- [33] Syahrul, S., *et al.*, Thermodynamic Modeling of Fluidized Bed Drying of Moist Particles, *International Journal of Thermal Science*, 42 (2003), 7, pp. 691-701
- [34] Tsotsas, E., From Single Particle to Fluid Bed Drying Kinetics, *Drying Technology*, 12 (1994), 6, pp. 1401-1426
- [35] Zahed, A. H., *et al.*, Modelling and Simulation of Batch and Continuous Fluidized Bed Dryers, *Drying Technology*, 13 (1995), 1-2, pp. 1-28
- [36] Burgschweiger, J., Tsotsas, E., Experimental Investigation and Modelling of Continuous Fluidized Bed Drying under Steady-State and Dynamic Conditions, *Chemical Engineering Science*, 57 (2002), 24, pp. 5021-5038
- [37] Kunii, D., Levenspiel, O., *Fluidization Engineering*, 2nd ed., Butterworth-Heinemann, Boston, Mass., USA, 1991
- [38] Patankar, S. V., *Numerical Heat Transfer and Fluid Flow*, Hemisphere P. C., New York, USA, 1980
- [39] Stakić, M., *et al.*, An Initial Study on Feasible Treatment of Serbian Lignite through Utilization of Low-Rank Coal Upgrading Technologies, *Chemical Engineering Research and Design*, 92 (2014), 11, pp. 2383-2395
- [40] Darton, R., *et al.*, Bubble Growth Due to Coalescence in Fluidized Beds, *Trans. Inst. Chem. Eng.*, 55 (1977), 4, pp. 274-280
- [41] Hirschmann, C., *et al.*, Comparison of Two Basis Methods for Measuring Drying Curves: Thin Layer Method and Drying Channel, *Proceedings*, 11th International Drying Symposium (IDS '98). Neos Marmaras, Greece, 1998, pp. 224-231
- [42] Tsotsas, E., *VDI-Warme-Atlas* (in German), 9th ed., Section Mh 6., Springer, Berlin, 2002
- [43] Gnielinski, V., *VDI-Warme-Atlas* (in German), 9th ed., Section Gj 1., Springer, Berlin, 2002
- [44] Oka, S. N., *Fluidized Bed Combustion*, Marcel Dekker, Inc., New York, Basel, Switzerland, 2003
- [45] Aziz, M., *et al.*, Innovative Energy-Efficient Biomass Drying Based on Self-Heat Recuperation Technology, *Chemical Engineering Technology*, 34 (2011), 7, pp. 1095-1103